Received: 24 May 2023 | Revised: 11 September 2023 | Accepted: 9 November 2023

DOI: 10.1111/jbg.12835

Journal of Animal Breeding and Genetics WILEY

ORIGINAL ARTICLE

Differential patterns in runs of homozygosity in two mice lines under divergent selection for environmental variability for birth weight

Candela Ojeda-Marín[1] | **Juan Pablo Gutiérrez**[1] | **Nora Formoso-Rafferty**[2] | **Félix Goyache**[3] | **Isabel Cervantes**[1]

[1]Departamento de Producción Animal, Facultad de Veterinaria, Universidad Complutense de Madrid, Madrid, Spain

[2]SERIDA-Deva, Gijon, Spain

[3]Departamento de Producción Agraria, E.T.S. Ingeniería Agronómica, Alimentaria y de Biosistemas, Universidad Politécnica de Madrid, Madrid, Spain

Correspondence
Candela Ojeda-Marín, Departamento de Producción Animal, Facultad de Veterinaria, Universidad Complutense de Madrid, Avenida Puerta del Hierro s/n 28040, Madrid, Spain.
Email: candelao@ucm.es

Funding information
Ministry of Science, Innovation, and Universities, Grant/Award Number: PGC2018-096198-A-I00

Abstract

Runs of homozygosity (ROH) are defined as long continuous homozygous stretches in the genome which are assumed to originate from a common ancestor. It has been demonstrated that divergent selection for variability in mice is possible and that low variability in birth weight is associated with robustness. To analyse ROH patterns and ROH-based genomic inbreeding, two mouse lines that were divergently selected for birth weight variability for 26 generations were used, with: 752 individuals for the high variability line (H-Line), 766 individuals for the low variability line (L-Line) and 74 individuals as a reference population. Individuals were genotyped using the high density Affymetrix Mouse Diversity Genotyping Array. ROH were identified using both the sliding windows (SW) and the consecutive runs (CR) methods. Inbreeding coefficients were calculated based on pedigree (F_{PED}) information, on ROH identified using the SW method (F_{ROHSW}) and on ROH identified using the CR method (F_{ROHCR}). Differences in genomic inbreeding were not consistent across generations and these parameters did not show clear differences between lines. Correlations between F_{PED} and F_{ROH} were high, particularly for F_{ROHSW}. Moreover, correlations between F_{ROHSW} and F_{PED} were even higher when ROH were identified with no restrictions in the number of heterozygotes per ROH. The comparison of F_{ROH} estimates between either of the selected lines were based on significant differences at the chromosome level, mainly in chromosomes 3, 4, 6, 8, 11, 15 and 19. ROH-based inbreeding estimates that were computed using longer homozygous segments had a higher relationship with F_{PED}. Differences in robustness between lines were not attributable to a higher homozygosis in the L-Line, but maybe to the different distribution of ROH at the chromosome level between lines. The analysis identified a set of genomic regions for future research to establish the genomic basis of robustness.

KEYWORDS

divergent selection, environmental birth weight variability, molecular inbreeding, runs of homozygosity

1 | INTRODUCTION

Inbreeding coefficients have been traditionally computed through pedigree information (Howard et al., 2017). However, inbreeding can be estimated using molecular information by assessing the homozygous sites. Given the strong relationship with genealogical inbreeding (McQuillan et al., 2008), runs of homozygosity (ROH) are continuous homozygous segments of DNA sequence (Ceballos et al., 2018) that are useful to quantify individual autozygosity. The intense selection of livestock has resulted in an increase of inbreeding. Moreover, the detection of common ROH regions in a population may not only result from genetic drift but may also become fixed in the population due to artificial selection. In addition, may reflect the population historical events as bottlenecks (Boyko et al., 2010; Kim et al., 2013; Sams & Boyko, 2019). It was, therefore, necessary to develop strategies to preserve genetic variability in populations and, to characterize and monitor autozygosity in animal breeding programmes (Peripolli et al., 2017).

The software program PLINK (Chang et al., 2015) is frequently used to analyse ROH in livestock populations such as cattle, sheep, swine, goat and horse (Peripolli et al., 2017). The algorithm in PLINK employs a sliding window approach for analysing the genome whereby users define some parameters. This window moves along the genome of an individual, detecting homozygous single nucleotide polymorphisms (SNPs) that, depending on the defined parameters, are part of a ROH (Meyermans et al., 2020). However, some reports indicate that the PLINK ROH algorithm may identify both artificial runs shorter than the fitted window or fail to identify segments longer than the window. Therefore, other algorithms were proposed to identify consecutive homozygous SNPs. A 'consecutive runs' algorithm can also enable the user to define a set of parameters to consider whether a homozygous SNP is part or not of a ROH (Ferenčaković et al., 2013; Marras et al., 2015).

New selection objectives relating to uniformity are becoming important in current animal breeding programmes (Marjanovic et al., 2016; Rönnegård et al., 2013; Vandenplas et al., 2013). Selecting to reduce the environmental variability of a particular trait has been shown to be possible (Blasco et al., 2017; Formoso-Rafferty et al., 2016a) with increasing importance in the breeding programmes of different livestock species (dos Santos Daltro et al., 2022; Garreau et al., 2008; Poyato-Bonilla et al., 2021). Selection for uniformity would result in animals more robust and better prepared to face environmental challenges (Broom, 2008). These are directly related to higher profitability and improvement in animal welfare (Bolet et al., 2007; Poigner et al., 2000). Recently, Casto-Rebollo et al. (2021) have shown that selection to modify the environmental variance of litter size involve genes with a functional mutation in their transcription units and are mostly implicated in the immune response and stress response pathways. More uniform animals would be less affected by unappreciable environments environment changes thus keeping their performance, which is a sign of robustness. In addition, it has been empirically confirmed that the more uniform the animals are the more robust they are.

In fact, Formoso-Rafferty et al. (2016a) developed a divergent selection experiment for birth weight variability in mice for 29 generations and concluded that it was possible to modify the genetic control of the birth weight environmental variability. As a result of the divergent experiment, two divergent lines were created: a high variability line (H-Line) and a low variability line (L-Line). The L-Line presented benefits in production, animal welfare, heritability and traits related with robustness traits such as feed efficiency or longevity (Formoso-Rafferty et al., 2016b, 2017, 2019, 2022; 2023). Moreover, a higher response to selection was observed in the L-Line than in the H-Line (Formoso-Rafferty et al., 2020).

The aim of this study was to analyse the variation of both patterns of ROH and ROH-based genomic inbreeding due to divergent selection in the two mouse lines. ROH-based inbreeding was estimated using different ROH lengths and two different algorithms: sliding windows and consecutive runs, and then compared with inbreeding coefficients computed using pedigree information within selection lines.

2 | METHODS

The experimental mouse population was created from a population originating from genetic contribution of three inbred mice lines: BALB/c, C57BL and CBA. This mixed starting population was maintained under panmixia for 40 generations and was the same as that used for the origin of other selection experiments (Fernández & Toro, 1999; Gutiérrez et al., 2006; Gutiérrez & Goyache, 2005; Ibáñez-Escriche et al., 2008; Moreno et al., 2012; Pun et al., 2013). A divergent selection experiment was designed and performed using the predicted breeding value for birth weight environmental variability as the selection criterion, which was considered as a trait of the mother. A total of 64 males and 64 females from the panmictic population were randomly selected to be mated one male to one female and that formed the founder population. Then, the pup weight and its environmental variability were considered as

maternal traits: A genetic selection was then carried out for low and high environmental variability. While avoiding mating between individuals that shared grandparents, mating was implemented using a simulated annealing approach to optimize the response to selection while restricting the increase in inbreeding (Formoso-Rafferty et al., 2016a).

2.1 | Data

Mouse tail samples were collected during 24 generations. A total of 1824 samples were genotyped using Affymetrix Mouse Diversity Genotyping Array, which included 616,316 SNPs. The Axiom Analysis Suite 3.1. (ThermoFisher Scientific) was used to extract genotypes and to create standard PED and standard map PLINK files. Quality control (QC) measures were then applied on the obtained genotypes. Animals with a call rate lower than 97% were removed. Finally, 752 females from the H-Line and 766 females from the L-Line were kept for this study. Furthermore, 74 females, including five females from the founder population and 69 from the first generation of selection, were used as a reference population (RP). Other QC measures were: 3% of missing genotypes were allowed but removed SNPs mapped in the sex chromosome and mitochondrial DNA. A minor allele frequency (MAF) filter was not applied to maximize the genome coverage calculated as recommended by Meyermans et al. (2020). Finally, 545,656 SNPs were kept, thus ensuring that 99% of the genome was covered.

The pedigree data contained 5054 individuals, including the 1592 individuals used this study and their ancestors up to five generations of pedigree of the founder population. The number of genotyped individuals per generation is given in Figure 1.

2.2 | Analysis

ROH were identified using two different algorithms: sliding windows (SW) as implemented by the PLINK v 1.9 program (Chang et al., 2015; Purcell et al., 2007) and consecutive runs (CR) (Ferenčaković et al., 2013; Marras et al., 2015) as implemented in the detectRuns package (Biscarini et al., 2018) of the R program. First, we tested different possibilities for each parameter involved in the computation of ROHs. We then decided to show only the variation in the number of heterozygotes allowed per ROH because we observed that this parameter is the most influential in the ROH detection in our data set—both in the number of segments detected and in the correlation between F_{ROH} and F_{PED}. The results of the other tests are not shown due to the final dimension of the article. The SW algorithm was fitted using the following parameters: 50 SNPs per window; one heterozygote site was allowed in a window; one heterozygote site was allowed per ROH; five missing SNPs were allowed in a window; a minimum ROH length of 1000 kb; the minimum number of homozygous SNPs in a ROH was set to 100; the required minimum density was set in one SNPs/50 kb; window threshold was set to 0.05; and the minimum distance between two ROHs was 1000 kb. The parameters fitted for CR were as follows: one heterozygote site allowed in a ROH; five missing SNPs allowed in a ROH; minimum ROH length of 1000 kb; the minimum number of homozygous SNPs in a ROH was set to 100; and the minimum distance between two ROH was 1000 kb.

Moreover, we also wanted to analyse how the selected number of heterozygotes affected the detection of ROH in these populations. For some of the computations in SW, no limit was set in the number of heterozygotes per ROH. SW with no limits in the heterozygotes per ROH labelled SW_0. When only one heterozygote was allowed per ROH, the SW label used was SW_1 and the CR label was CR_1.

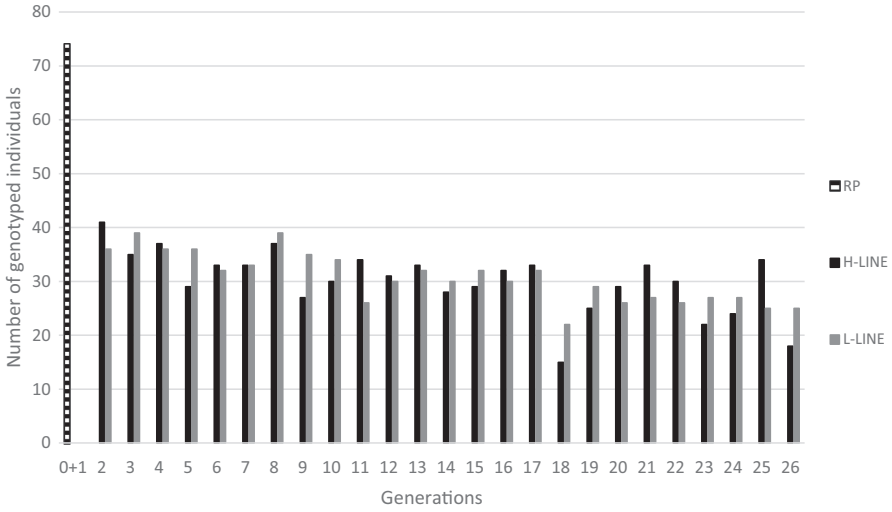

FIGURE 1 Number of genotyped individuals per generation in the high variability line (H-Line), in the low variability line (L-Line) and in the reference population (RP) formed by individuals of generation 0 and of the first generation of selection.

Genomic inbreeding was computed as $F_{\mathrm{ROH}_i} = \frac{\sum L_{\mathrm{ROH}}}{L_{\mathrm{AUTO}}}$

where L_{ROH} was the total length of all ROH segments and L_{AUTO} was the autosomal genome distance covered by SNPs (2,458,711,710 bp) (McQuillan et al., 2008). Eight different F_{ROH} coefficients were calculated for each animal depending on the ROH length: $F_{\mathrm{ROH\ 1–2Mb}}$, $F_{\mathrm{ROH\ 2–4Mb}}$, $F_{\mathrm{ROH\ 4–8Mb}}$, $F_{\mathrm{ROH\ 8–12Mb}}$, $F_{\mathrm{ROH\ 12–16Mb}}$, $F_{\mathrm{ROH\ 16–20Mb}}$, $F_{\mathrm{ROH\ 20–26Mb}}$ and $F_{\mathrm{ROH\ 26–32Mb}}$. Where *x*–*y* Mb was the minimum and maximum length (in Mb) of the ROH used for computations. Furthermore, F_{ROH} coefficients were calculated into accumulative classes: $F_{\mathrm{ROH>1Mb,}}$ $F_{\mathrm{ROH>2Mb}}$, $F_{\mathrm{ROH>4Mb}}$, $F_{\mathrm{ROH>8Mb}}$, $F_{\mathrm{ROH>12Mb}}$, $F_{\mathrm{ROH>14Mb}}$, $F_{\mathrm{ROH>20Mb}}$, $F_{\mathrm{ROH>26Mb}}$ and $F_{\mathrm{ROH>32Mb}}$, with $F_{\mathrm{ROH>1Mb}}$ being equivalent to F_{ROH_i} as defined above.

Genealogical inbreeding (F_{PED}) is the probability that an individual had two identical alleles by descent and was computed following Meuwissen and Luo (1992) using the program ENDOG v4.9 (Gutiérrez & Goyache, 2005).

To compare the evolution of genealogical inbreeding and molecular inbreeding, individual inbreeding coefficients were standardized by the mean inbreeding coefficient of the RP as: $F_{xsi} = \frac{(F_{xi} - F_{xRP})}{1 - F_{xRP}}$; where *x* is $\mathrm{ROH_{SW1}}$, $\mathrm{ROH_{CR1}}$, $\mathrm{ROH_{SW0}}$ or PED and *i* is the individual. The standardized inbreeding coefficients are, therefore, labelled F_{ROHSW1s}, F_{ROHCR1s}, F_{ROHSW0s} and F_{PED}.

The Pearson correlation coefficient between the different inbreeding measures was estimated for both selected lines using the R program. F_{ROH}–F_{PED} correlations were also calculated in different generation groups: initial generations (2, 3, 4 and 5), intermediate generations (13, 14, 15 and 16) and the most recent generations (23, 24, 25 and 26). We carried out correlations in different generation groups with the algorithm and parameters that showed the best correlations between F_{PED}–F_{ROH} using all the individuals of the selected lines. These were done to clear up if there were differences in F_{PED}–F_{ROH} correlation across the selection generations and to compare correlations of a few numbers of individuals with correlations of all the genotyped individuals.

Consensus regions were defined as ROH regions within each selected line that were detected in the 99% of the analysed individuals and with a 99% of allelic match. These consensus regions were analysed in initial, intermediate and most recent generations to observe whether there were differences between lines and the evolution across generations. PLINK v1.9 was used to detect these regions (Chang et al., 2015; Purcell et al., 2007).

Furthermore, we calculated F_{ROH} within each chromosome (F_{ROHchr}) with the method and the parameters that best correlated with F_{PED} to identify differences in F_{ROH} in each chromosome between lines. We also calculated F_{ROHchr} in different generation groups: initial generations, intermediate generations and most recent generations. We then compared L-Line and H-Line to identify differences due to selection at the chromosome level. F_{ROHchr} that was computed for both the intermediate and the most recent generations of both selection lines was used to account for drift: Differences were consistently assessed in intermediate and most recent generations and considered likely to be linked to selection rather than genetic drift. To deal with this objective, F_{ROHchr} in each chromosome and in each generation group were analysed using a general linear model procedure with equation: $y = \mu + \mathrm{line} + e$, where *y* was the individual's F_{ROHchr} in the analysed chromosome, μ was the mean, *line* the selection line with two levels (H-Line and L-Line) and *e* the residual. The R package *car* (Fox & Weisberg, 2019) was used to perform the statistical analysis of the data.

2.3 | Candidate ROH regions

Chromosomes with statistically significant differences in F_{ROHchr} between lines, in both intermediate and most recent generations, and the line that presented more F_{ROHchr} in both generation groups were considered as harbouring candidate ROH regions. We defined ROH candidate regions as chromosome regions identified in 99% of the individuals belonging to the intermediate generations and most recent generations of both lines in two different scenarios:

(i) ROH regions exclusive of the L-Line not identified in the other selection line.
(ii) ROH regions exclusive of the H-Line not identified in the other selection line.

These scenarios were designed to test the hypothesis of dominant inheritance. In one of the lines, only one of the alleles was fixed and in the other line heterozygotes were also selected.

3 | RESULTS

Descriptive statistics of ROH are given in Table 1 that were identified under $\mathrm{SW_1}$, $\mathrm{CR_1}$ and $\mathrm{SW_0}$ in both selection lines and in the RP. The L-Line had more ROH segments than the H-Line under both methodologies and irrespective of any restrictions in the number of allowed heterozygotes per ROH. However, the identified mean number of segments was similar between lines: 338 for the H-Line and 336 for the L-Line under $\mathrm{SW_1}$, 335 for

TABLE 1 Descriptive statistics of runs of homozygosity number and length obtained by sliding windows (SW_1) and consecutive runs (CR_1) when one heterozygote was allowed per ROH and sliding windows when no restriction in the number of heterozygotes per ROH was set (SW_0) in the reference population (RP), in the high variability line (H-Line) and in the low variability line (L-Line).

	Number of segments	Mean number of segments per individual (SE)	Mean length of segments (Mb) (SE)	Maximum length of segments (Mb)
H-Line				
SW_1	274,060	338 (1.63)	4.20 (0.01)	90.46
CR_1	273,489	335 (2.54)	4.50 (0.01)	89.07
SW_0	220,123	293 (0.62)	5.55 (0.02)	136.50
L-Line				
SW_1	276,777	336 (1.44)	4.17 (0.01)	80.14
CR_1	276,665	336 (2.36)	4.40 (0.01)	82.64
SW_0	228,880	299 (0.59)	5.35 (0.01)	153.90
RP				
SW_1	29,430	327 (2.38)	3.79 (0.02)	63.54
CR_1	29,300	322 (4.60)	4.04 (0.02)	64.59
SW_0	21,290	288 (1.29)	4.62 (0.03)	99.89

Abbreviation: SE, standard error.

TABLE 2 Percentage of the total sum of ROH per length of ROH segment in the high variability line (H-Line), in the low variability line (L-Line) and in the reference population (RP). ROH were obtained using the sliding windows (SW_1) and the consecutive runs (CR_1) approaches when one heterozygote was allowed per ROH and using sliding windows when no restriction in the number of heterozygotes per ROH was set (SW_0).

	H-Line SW_1 (%)	H-Line CR_1 (%)	H-Line SW_0 (%)	L-Line SW_1 (%)	L-Line CR_1 (%)	L-Line SW_0 (%)	RP SW_1 (%)	RP CR_1 (%)	RP SW_0 (%)
1–2 Mb	12.91	11.58	8.56	13.25	12.20	8.98	14.98	12.94	10.90
2–4 Mb	20.59	19.82	14.15	19.82	19.80	15.25	23.54	22.25	18.43
4–8 Mb	26.68	26.41	20.58	26.41	26.57	20.97	28.43	28.61	24.30
8–12 Mb	15.45	16.09	13.34	16.09	16.61	14.76	15.59	17.19	15.96
12–16 Mb	8.57	9.56	9.34	9.56	9.29	9.06	7.82	8.70	9.51
16–20 Mb	5.81	6.50	8.18	6.50	6.20	7.64	3.90	4.40	6.65
20–26 Mb	4.65	4.96	7.45	4.96	4.80	6.86	3.08	3.47	5.08
26–32 Mb	2.42	2.57	5.08	2.08	2.41	4.86	1.44	1.29	3.05
≥32 Mb	2.94	2.49	13.29	2.66	2.12	10.59	1.23	1.16	6.13

the H-Line and 336 for the L-Line under CR_1 and 293 for the H-Line and 299 for the L-Line under SW_0. The mean and the maximum ROH lengths were greater in the selection lines than in the RP. The longest segment detected in RP under SW_1 was 63.54 Mb, under CR_1 it was 64.59 Mb and under SW_0, it was 99.89. In contrast, the longest segment in the H-Line was 90.46 Mb under SW_1, 89.07 Mb under CR_1 and 136.50 Mb under SW_0. And in the L-Line, it was 80.14 under SW_1, 82.64 Mb under CR_1 and 132.22 Mb under SW_0. A greater number of segments were detected using SW_1 and CR_1 rather than using SW_0, whereas the mean length and the maximum length of the segment were larger under SW_0 in both selected lines and in the RP.

Table 2 shows ROH segments with a length between 1 and 12 Mb were more frequent. In the H-Line, those segments were 75.63% in total, in the L-line, they were 76.44% of the total and in the RP, they amounted to 82.54% of the total under SW_1. Moreover, for CR_1 in the H-Line, those segments were 73.90% of the total identified, in the L-Line, they were 75.18% of the total and in the RP, they amounted to 80.99% of the total. For SW_0, the segment lengths between 1 and 12 Mb represented 56.63% in the H-Line, 59.96% in the L-Line and 69.59% in the RP. ROH segments between 4 and 8 Mb were the most frequent: 26.68% (H-Line), 26.41% (L-Line) and 28.43% (RP) under the SW_1 algorithm. Under the CR_1 approach segments between 4 and 8 Mb were 26.57% (L-Line), 26.41% (H-Line)

and 28.61% (RP). Furthermore, under SW_0, segments between 4 and 8 Mb represented 20.58% (H-Line), 20.97% (L-Line) and 24.30% (RP). RP had the lowest percentage of segments longer than 32 Mb: 1.23% under SW_1, 1.16% under CR_1 and 6.13% under SW_0. These percentages were 2.94% under SW_1, 2.49% under CR_1 and 13.29% under SW_0 for the H-Line and 2.66% under SW_1, 2.12% under CR_1 and 11.57% under SW_0 for the L-Line. When both algorithms were compared, SW_1 and CR_1 showed a similar proportion of segments in each class. Nevertheless, SW_0, as excepted, detected the highest percentage of segments longer than 16 Mb in both the selected lines and in the RP.

Figure 2 shows the evolution of F_{PEDs}, $F_{ROHSW1s}$, $F_{ROHCR1s}$ and $F_{ROHSW0s}$ across generations in both lines. The four parameters had a positive trend. In the last generation, the average for these parameters, F_{PEDs}, $F_{ROHSW1s}$, $F_{ROHCR1s}$ and $F_{ROHSW0s}$, were respectively: 0.34, 0.26, 0.27 and 0.31 for the H-Line. And for the L-Line: 0.34, 0.23, 0.25 and 0.28 respectively. More differences were detected in the evolution of $F_{ROHSW1s}$, $F_{ROHCR1s}$ and $F_{ROHSW0s}$ than in F_{PED} for the selected lines. The L-Line presented a noticeable decrease in the 25th generation in F_{ROHSW1} (0.16) and F_{ROHCR1} (0.17). This decrease was not observed in F_{ROHSW0} (0.28). In RP, F_{ROHSW1} was 0.50, F_{ROHCR1} was 0.53, F_{ROHSW0} was 0.54 and for F_{PED}, it was 0.03.

The variation of F_{ROH} per ROH length classes and algorithm (SW_1, CR_1 and SW_0) in both selection lines is shown in Figure S1. When F_{ROH} was calculated using segments greater than 12 Mb, F_{ROHSW1} and F_{ROHCR1} calculated by segments between 12 and 16 Mb explained more F_{ROH} than larger segments in both selection lines (see Figure S1b,d). However, F_{ROHSW0} obtained from segments longer than 32 Mb contributed more to F_{ROH} than segments between 12 and 32 Mb in both selection lines (see Figure S1). Nevertheless, segments between 4 and 8 Mb explained most of F_{ROH} across methods and restrictions.

The correlation of F_{PED} with F_{ROH} calculated with information from all the genotyped animals across generations computed using SW_1 were: 0.85 in the H-Line and the L-Line, and 0.11 in the RP. These correlations computed using CR_1 were 0.78 in the H-Line, 0.80 in the L-Line and 0.13 in the RP. When SW_0 was used to calculate ROH, correlations between F_{PED} and total F_{ROH}, these were 0.89 in the H-Line, 0.88 in the L-Line and 0.12 in the RP. Figure 3 shows the correlations between F_{PED} and F_{ROHSW1}, F_{ROHCR1} and F_{ROHSW0} that were calculated using different ROH length and accumulative length classes for both selection lines and the RP. In general, correlation coefficients were highest for the pair F_{PED}–F_{ROHSW0}, and F_{ROHSW1}–F_{PED} correlations were

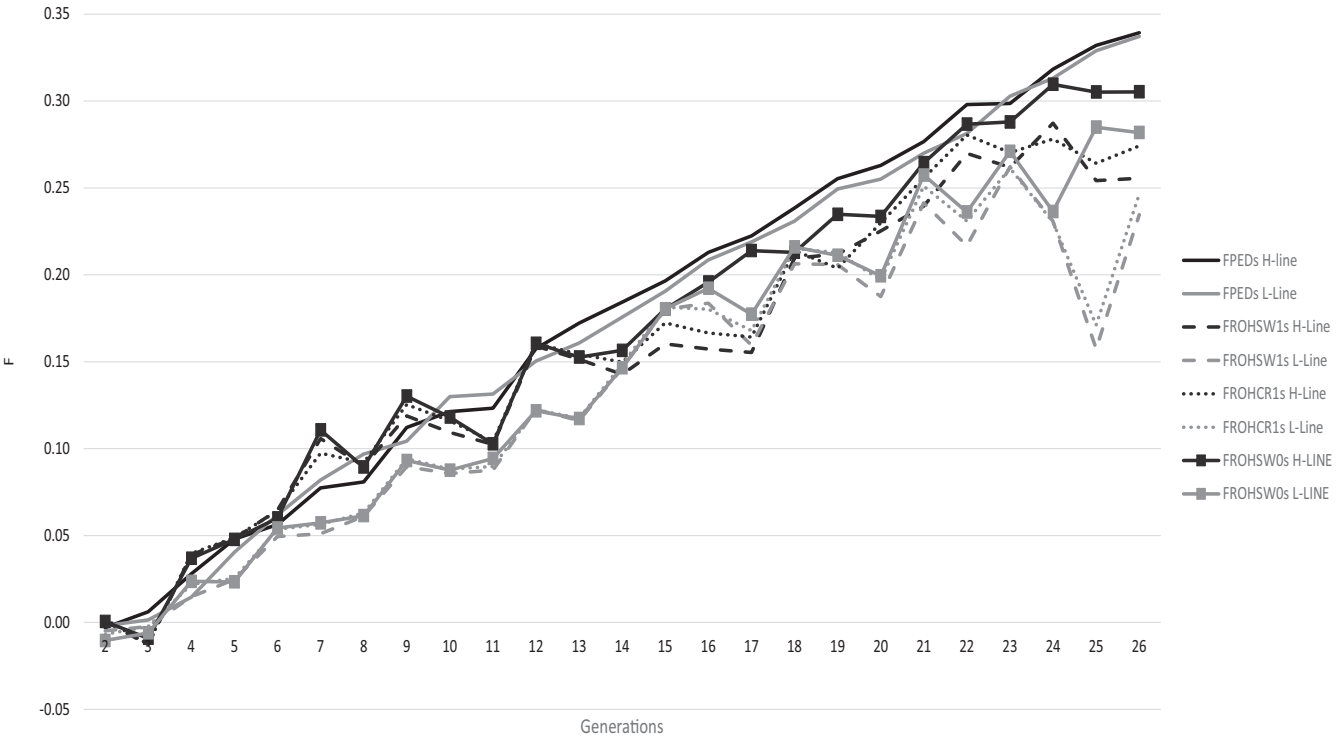

FIGURE 2 Evolution of average inbreeding coefficients adjusted by the average inbreeding of the reference population based on pedigree (F_{PEDs}) and genomic inbreeding calculated by sliding windows ($F_{ROHSW1s}$) and consecutive runs ($F_{ROHCR1s}$) when one heterozygote was allowed per ROH and sliding windows when no restriction in the number of heterozygotes per ROH was set ($F_{ROHSW0s}$); in high variability line (H-Line) and low variability line (L-Line). H-Line: black, L-Line: grey.

higher than F_{ROHCR1}–F_{PED} correlations. The lowest correlations were observed when segments between 1 and 4 Mb were used to calculate F_{ROH} (Figure 3a); the pairs $F_{ROHSW0\ 1–2\ Mb}$–F_{PED} and $F_{ROHSW0\ 2–4\ Mb}$–F_{PED} showed the lowest correlations (Figure 3b). Furthermore, using ROH segments ≥2 Mb length, the correlation coefficients were 0.88 in both selected lines for SW_0 approach, 0.69 and 0.58 in the H-Line, and 0.69 and 0.56 in L-Line for the SW_1 and the CR_1 approaches. The correlations between F_{ROH} and F_{PED} when segments longer than 32 Mb were used, remained higher with: SW_0 (0.57 in the H-Line and 0.63 in the L-Line) than with SW_1 (0.23 in the H-Line and 0.25 in the L-Line) and with CR_1 (0.22 in the H-Line and 0.24 in the L-Line). Regardless of the selection line or algorithm considered, the shorter length of ROH used for computations, the lower the correlation coefficients with F_{PED}. This decrease was not observed in RP.

We observed an irregular pattern in the correlations of H-Line and L-Line in the different group of generations when using different algorithms and restrictions. Correlation coefficients reached values from moderate to low when only a few generations were considered. When cumulative categories were considered to calculate F_{ROHSW0}, correlations were positive in all the generation groups and higher in the intermediate generations (see Figure S2).

The evolution of consensus regions in the H-Line and L-Line detected in initial, intermediate and most recent generations are represented in Figure 4. With the generations pass, more consensus regions were detected in both lines. The greatest difference between lines were observed in intermediate generations, where the H-Line presented 175 consensus regions and the L-Line presented 191 consensus regions. Table S1 shows all the consensus regions

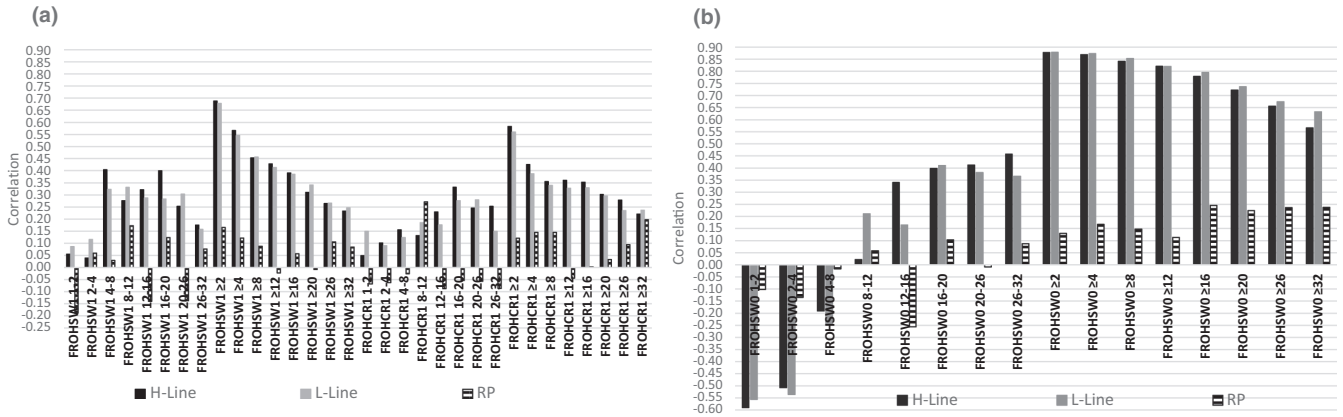

FIGURE 3 Correlations between pedigree inbreeding (F_{PED}) and genomic inbreeding calculated by runs of homozygosity (ROH) computed using sliding windows setting one heterozygote per ROH (F_{ROHSW1}), consecutive runs (F_{ROHCR1}) and sliding windows setting no restrictions in the number of heterozygotes allowed by ROH (F_{ROHSW0}) in both divergent lines and in the reference population. F_{ROHSW1}, F_{ROCR1} and F_{ROHSW0} are divided in eight classes (1–2, 2–4, 4–8, 8–12, 12–16, 16–20, 20–26 and 26–32 Mb) and in eight cumulative categories (≥2, ≥4, ≥8, ≥12, ≥16, ≥20, ≥26 and ≥32 [Mb]). Plot (a) represented F_{PED}–F_{ROHSW1} and F_{PED}–F_{ROHCR1} correlations. Plot (b) represented F_{PED}–F_{ROHSW0} correlations. High variability line: black. Low variability line: grey. Reference population: striped black.

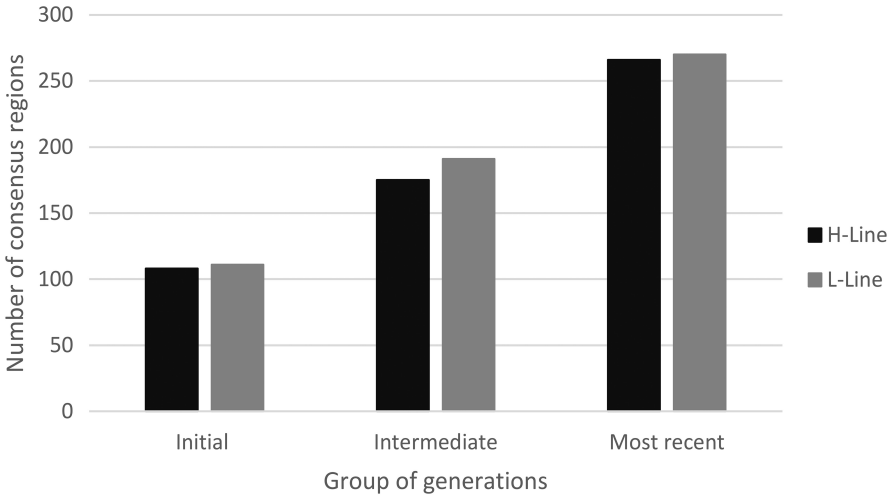

FIGURE 4 Number of consensus regions in different groups of generations: initial (2, 3, 4 and 5), intermediate (13, 14, 15 and 16) and most recent (23, 24, 25 and 26) generations, detected in low variability line (L-Line) and high variability line (H-Line).

detected per line and per group of generations. Some differences were observed in chromosome distribution between lines, for instance, consensus regions in chromosome 19 were detected from the initial generations in the H-Line while in the L-Line they were not detected until the most recent generations.

Table 3 shows the mean and the standard error of F_{ROHchr} in H-Line and L-Line in intermediate and most recent generation groups. Moreover, also shown is the significance in differences in the F_{ROHchr} between lines in intermediate and most recent generations. Consistent significant differences were detected in chromosomes 3, 4, 6, 8, 11, 15 and 19 in intermediate and recent generations. Only chromosome 3 presented greater F_{ROHchr} in the L-Line; 0.54 in H-Line and 0.60 in L-Line in intermediate generations and 0.62 in the H-line and 0.70 in the L-Line in most recent generations. Chromosomes 4, 6, 8, 11 and 15 presented greater F_{ROHchr} in the-H Line. In chromosome 4: F_{ROHchr} was 0.62 in the H-Line and 0.58 in the L-Line in intermediate generations; and 0.66 in the H Line and the 0.58 in L-Line in most recent generations. In chromosome 6, this was: 0.77 in H-Line and 0.64 in L-Line for the intermediate generations; and 0.83 in the H-Line and 0.65 in the L-Line in most recent generations. In the intermediate generations, chromosome 8 for the: H-Line had 0.69 and 0.63 for the L-Line; and in the most recent generations, the H-Line had 0.73 and 0.65 for the L-Line. In chromosome 11, in the intermediate generations: F_{ROHchr} was 0.53 for the H-line and 0.48 for the L-Line; and 0.61 for the L-Line and 0.54 for the L-Line in most recent generations. In chromosome 15 for the intermediate generations: F_{ROHchr} was 0.69 in the H-Line and 0.56 in in the L-Line; and 0.75 for the H-Line and 0.64 for the L-Line in the most recent generations. Finally, in chromosome 19: F_{ROHchr} was 0.50 in H-Line and 0.47 in L-Line in intermediate generations; and 0.60 in H-Line and 0.53 in L-Line in most recent generations.

Candidate regions exclusive to the H-line covered 84,490,502 bp of the mice genome, with a total of 176 regions: 36 of which were identified in chromosome 4; 30 in chromosome 6, 26 in chromosome 8; 35 in chromosome 11, 28 in chromosome 15 and 21 in chromosome 19. Candidate regions exclusive to the L-Line covered 21,645,521 bp of the mice genome, with a total of 55 regions all of which were detected in chromosome 3. The longest candidate region exclusive to the H-Line was detected in chromosome 15 (4,985,142 bp), and the longest candidate region exclusive to the L-Line was detected in chromosome 3 (2,219,748 bp) (see Table S2).

TABLE 3 Mean and standard error (SE) of ROH inbreeding computed using sliding windows per chromosome with no restrictions in the number of heterozygotes allowed per ROH (F_{ROHchr}). Significance of differences in F_{ROHchr} for the selection line effect compared between intermediate generations (13, 14, 15 and 14) and most recent generations (23, 24, 25 and 26).

	Intermediate generations				Most recent generations			
	H-Line		L-Line		H-Line		L-Line	
Chromosome	Mean	SE	Mean	SE	Mean	SE	Mean	SE
1	0.59	0.01	0.57	0.01	0.61***	0.01	0.69***	0.01
2	0.66**	0.01	0.69**	0.01	0.67	0.01	0.68	0.01
3	0.54***	0.01	0.60***	0.01	0.63***	0.01	0.71***	0.01
4	0.62**	0.01	0.58**	0.01	0.66***	0.01	0.58***	0.01
5	0.65***	0.01	0.68***	0.01	0.71	0.01	0.72	0.01
6	0.77***	0.01	0.64***	0.01	0.83***	0.01	0.65***	0.01
7	0.55	0.01	0.57	0.01	0.62	0.01	0.62	0.01
8	0.69**	0.01	0.63**	0.01	0.73***	0.01	0.65***	0.01
9	0.59	0.01	0.62	0.01	0.61***	0.01	0.71***	0.01
10	0.76	0.01	0.75	0.01	0.79	0.01	0.79	0.01
11	0.53***	0.01	0.48***	0.01	0.61***	0.01	0.54***	0.01
12	0.54***	0.01	0.60***	0.01	0.64	0.01	0.66	0.01
13	0.60***	0.01	0.65***	0.01	0.66	0.01	0.70	0.01
14	0.66	0.01	0.65	0.01	0.79***	0.01	0.66***	0.01
15	0.69***	0.01	0.56***	0.01	0.75***	0.01	0.64***	0.01
16	0.63	0.01	0.63	0.01	0.69	0.01	0.69	0.01
17	0.54	0.01	0.54	0.01	0.61	0.01	0.64	0.01
18	0.55***	0.01	0.62***	0.01	0.64	0.01	0.65	0.01
19	0.50*	0.01	0.47*	0.01	0.60***	0.01	0.53***	0.01

*$p < 0.05$; **$p < 0.01$; ***$p < 0.001$.

4 | DISCUSSION

Since high levels of inbreeding produce an increase in the frequency of homozygous alleles, ROH have become useful to estimate inbreeding (Peripolli et al., 2017). Selection pressure and mating schemes can influence ROH length and distribution in the genome causing a non-random distribution of these genomic features. Therefore, ROH detection can also be used to minimize inbreeding and to improve mating systems (Mastrangelo et al., 2018).

ROH studies have been performed in many other species such as cattle (Caivio-Nasner et al., 2021; Doekes et al., 2019; Lozada-Soto et al., 2022; Marras et al., 2015; Peripolli et al., 2020; Pryce et al., 2014; Purfield et al., 2012; Schiavo et al., 2022; Zhang et al., 2015), pigs (Ganteil et al., 2020; Joaquim et al., 2019; Saura et al., 2015; Schäler et al., 2020; Schiavo et al., 2020), sheep (Álvarez et al., 2020; Nosrati et al., 2021; Rodríguez-Ramilo et al., 2019), horses (Bizarria dos Santos et al., 2021; Druml et al., 2018; Grilz-Seger et al., 2019), goats (Cortellari et al., 2021; Onzima et al., 2018; Signer-Hasler et al., 2022), poultry (Elbeltagy et al., 2019; Marchesi et al., 2018), turkeys (Strillacci et al., 2020), dogs (Mastrangelo et al., 2018; Mooney et al., 2021; Sams & Boyko, 2019; Soh et al., 2021) and salmon (Yoshida et al., 2020). However, both within and between species, the comparison between studies is challenging because the density of the available genotypes and the high variability of the parameters fitted to identify ROH (Peripolli et al., 2017; Rodríguez-Ramilo et al., 2019).

Therefore, the authors cannot agree what parameters and algorithms to use to identify the ROH. This makes it difficult to compare results from different studies (Peripolli et al., 2017). In addition, there are few studies aimed at evaluating the impact of fitting different parameters in the performance of the algorithms used to identify ROH. This also affects the estimation of F_{ROH} (Biscarini et al., 2018; Ferenčaković et al., 2013; Howrigan et al., 2011; Meyermans et al., 2020; Mulim et al., 2022; Rodríguez-Ramilo et al., 2019). To optimize ROH detection as recommended by Meyermans et al. (2020), the MAF thresholds and linkage disequilibrium pruning were not applied in this study. These authors reported losses of ROH information when these filters were applied on genotype data.

In this study, segments between 1 and 12 Mb of length identified under both SW_1 and CR_1 were highly consistent. These ROH segments played a major contribution to the total sum of ROH, as reported for other species: cattle (Ferenčaković et al., 2013; Marras et al., 2015), horse (Grilz-Seger et al., 2019), swine (Saura et al., 2015; Schiavo et al., 2020) or dogs (Mastrangelo et al., 2018). The performance of both algorithms can be considered highly consistent for many practical purposes. Other authors (Bertolini et al., 2018) have estimated that ROH shorter than 8 Mb originated from ancestors living more than six generations before, whereas ROH segments longer than 16 Mb originated from ancestors living less than three generations before. Furthermore, Howrigan et al. (2011) estimated that the ROH lengths of 10 Mb, 5 Mb and 2.5 Mb would, respectively, originate from ancestors living 5, 10 and 20 generations before. Similar distances from ancestors were reported by Curik et al. (2014). Hence, most of the segments detected in both selection lines and in the RP with both algorithms could be generated more than six generations previously and might be related to ancient inbreeding. Moreover, the RP had a lower proportion of segments longer than 12 Mb suggesting that this population would have lower levels of recent inbreeding. However, it is worth mentioning that not all ROH originated in identity-by-descent events. Some ROH could be located in genomic regions showing a low recombination rate and high linkage disequilibrium present in individuals that might not share common ancestors, therefore, considered identical-by-state (Purfield et al., 2017).

In this study, the total F_{ROH} ($F_{ROH\geq 1\,Mb}$) had higher correlations with F_{PED}. This is consistent with previous reports in other populations, such as: Iberian pig 0.63 (Saura et al., 2015), cattle 0.75 (Marras et al., 2015), sheep 0.76 (Purfield et al., 2017), goat 0.64–0.88 (Bertolini et al., 2018) and even human 0.86 (McQuillan et al., 2008). Our results confirm that F_{ROH} can be considered a good measure of the individual inbreeding. Nevertheless, it should be noted that they were in the extreme of the reported range given that the genotypes belonged to a considerable number of different generations. Thus, probably influencing the appearance of such higher correlation between total F_{ROH} and F_{PED} in both divergent selection lines. This was supported by the fact that correlations between F_{PED} and F_{ROH} were lower when generation groups were considered (Figure 4). Some authors reporting moderate to low correlations between F_{PED} and F_{ROH} justified their findings to a shallow pedigree available to them (Biscarini et al., 2020; Purfield et al., 2017; Schiavo et al., 2022). Hence, the moderate to high correlations between F_{PED} and F_{ROH} computed in this study when all the available generations were considered was likely to be explained by both the presence of a deep enough pedigree and the high variability of inbreeding coefficients across generations. Furthermore, when the performance of the algorithms was compared, SW gave higher correlations between F_{PED} and F_{ROH} and, therefore, should be preferred in our population. In fact, when no restrictions in the number of heterozygotes per ROH were set, SW tended to give the highest correlations,

except for segments between 1 and 8 Mb. Some authors recommended no heterozygous calls per ROH (Ceballos et al., 2018; Howrigan et al., 2011). However, Ferenčaković et al. (2013) suggested that genotyping errors in SNP chip data do occur and, therefore, by not allowing heterozygous calls can make shorter segments. These authors also suggested that the number of heterozygous sites allowed per ROH should be adapted to the length of the target ROH segments. Nevertheless, in the available software, there is no option for setting the number of heterozygotes sites as a function of the ROH length. Furthermore, other authors (Aramburu et al., 2020; Biscarini et al., 2020) reported that allowing one heterozygote per sliding window enables the identification of a higher proportion of longer ROH when compared to not allowing heterozygotes per window, as the findings of this study confirm (Table 2; Figure S1). Furthermore, they suggested that allowing heterozygotes sites should be considered in function of both the sequencing technology and the marker density to avoid the mistaken break of ROH. Therefore, although other authors used CR instead of SW to avoid the identification of spurious ROH (Ferenčaković et al., 2013), F_{ROHSW1} correlated better than F_{ROHCR1} in our case. When no restrictions were fitted in the number of heterozygotes per ROH (SW_0), the correlations between F_{PED} and F_{ROH} were even higher. Moreover, when increasing the minimum length for calculating F_{ROH}, correlations were still the highest between F_{PED} and F_{ROHSW0}. This was probably because SW_0, adapted better to the presence of heterozygote sites in function of the ROH length and, because of a lower number of wrongly broken ROH. When the heterozygotes were set by a sliding window and not per ROH.

Saura et al. (2015) reported negative correlations using sliding windows between $F_{ROH<5\ Mb}$ and F_{PED} suggesting that these negative correlations should be interpreted with caution. Although shorter ROH are likely to have originated from remote common ancestors, they could be covered or included in some of the longer ROH. Therefore, although longer ROH were associated with recent inbreeding (Howrigan et al., 2011; Rodríguez-Ramilo et al., 2019), the amount of recent and old inbreeding mirrored in each ROH segment might be affected by other factors rather than their length such as: population size, mating system or selection pressure. Hence, in our closed population, it is likely that longer ROH segments better depict identity-by-descent events than shorter segments due to both the high selection pressure applied and the low number of mating animals per generation.

In any case, comparison between ROH-based genomic inbreeding parameters and genealogical inbreeding is not straightforward. Pedigree inbreeding is the expected proportion of the genome that is identical by descent and, therefore, cannot capture the variation caused by other forces, such as Mendelian sampling or the linkage disequilibrium in the gamete formation, that are different to matings between relatives (Howard et al., 2017; Rodríguez-Ramilo et al., 2019).

Differences in trends of both pedigree and molecular inbreeding were not high between lines. Some authors developed models by assuming that the residual variance decreases when the number of homozygous *loci* increases (Lerner, 1954; Lewontin, 1964; Zhivotovsky & Feldman, 1992). In any case, the current results suggest that selection for low variability of birth weight do not cause a higher increase of homozygosity in the L-Line when compared with the H-Line. The highest difference between lines in molecular inbreeding occurred in the 25th generation when using SW_1 and CR_1. This decrease was not observed when SW_0 was used, that had the highest correlations with F_{PED} in both selected lines and possibly be more representative of identity by descent in these lines. Currently, there is no convincing or conclusive explanation for the decrease observed using SW_1 and CR_1, which is still being investigated, but a sampling effect, together with the parameter criteria used to detect the ROH regions, might play an important role here. Nevertheless, ROH presented a different consensus regions distribution pattern between lines across chromosomes. Moreover, the differences in F_{ROHchr} detected in chromosomes 3, 4, 6, 8, 11, 15 and 19 made it possible to identify candidate ROH regions, also known as ROH islands or ROH hotspots in other species (Biscarini et al., 2020; Caivio-Nasner et al., 2021; Grilz-Seger et al., 2019; Lozada-Soto et al., 2022; Peripolli et al., 2020; Rodríguez-Ramilo et al., 2021; Schiavo et al., 2022; Signer-Hasler et al., 2022; Yoshida et al., 2020), that could be the result of selection and be implicated in the different performance between lines. This question is currently under investigation together with other methodologies specifically designed to find candidate genes.

5 | CONCLUSIONS

Estimates of F_{ROH} and F_{PED} had from moderate to high correlation. However, they correlated better for the SW approach, and when no restriction was set in the number of heterozygotes per ROH to identify ROH. The use of the same heterozygote restriction per ROH regardless of the size of the segment could mistakenly break the ROH segments. ROH-based molecular inbreeding was better represented by longer segments in these populations. Differences in robustness between the low variability line

and the high variability line were not likely to be caused by differences in the total amount of genomic homozygosis. Nevertheless, different distribution of ROH in chromosomes may underlie performance differences between lines that are candidate ROH regions. The genomic regions identified in chromosomes 3, 4, 6, 8, 11, 15 and 19 can be a target for future research aimed at establishing the genomic basis of robustness.

ACKNOWLEDGEMENTS

The genotyping service was carried out at CEGEN-PRB3-ISCIII; it is supported by grant PT17/0019, of the PE I+D+i 2013–2016, and funded by ISCII and ERDF.

FUNDING INFORMATION

This study was funded by a grant from the Ministry of Science, Innovation and Universities; grant number: PGC2018-096198-A-I00.

CONFLICT OF INTEREST STATEMENT

The authors declare no conflicts of interest.

DATA AVAILABILITY STATEMENT

The data sets analysed during this study are available from the corresponding author upon reasonable request.

ORCID

Candela Ojeda-Marín https://orcid.org/0000-0002-7213-4089
Juan Pablo Gutiérrez https://orcid.org/0000-0003-3142-2356
Nora Formoso-Rafferty https://orcid.org/0000-0003-2319-3485
Félix Goyache https://orcid.org/0000-0002-6872-1045
Isabel Cervantes https://orcid.org/0000-0002-0750-6480

REFERENCES

Álvarez, I., Fernández, I., Traoré, A., Pérez-Pardal, L., Menéndez-Arias, N. A., & Goyache, F. (2020). Ancient homozygosity segments in West African Djallonké sheep inform on the genomic impact of livestock adaptation to the environment. *Animals*, *10*, E1178.

Aramburu, O., Ceballos, F., Casanova, A., Le Moan, A., Hemmer-Hansen, J., Bekkevold, D., Bouza, C., & Martínez, P. (2020). Genomic signatures after five generations of intensive selective breeding: Runs of homozygosity and genetic diversity in representative domestic and wild populations of turbot (*Scophthalmus maximus*). *Frontiers in Genetics*, *11*, 296.

Bertolini, F., Cardoso, T. F., Marras, G., Nicolazzi, E. L., Rothschild, M. F., & Amills, M. (2018). Genome-wide patterns of homozygosity provide clues about the population history and adaptation of goats. *Genetics Selection Evolution*, *50*, 59.

Biscarini, F., Cozzi, P., Gaspa, G., & Marras, G. (2018). An R package to detect runs of homozygosity and heterozygosity in diploid genomes. In *CRAN 'The Compr. R Arch. Network'*.

Biscarini, F., Mastrangelo, S., Catillo, G., Senczuk, G., & Ciampolini, R. (2020). Insights into genetic diversity, runs of homozygosity and heterozygosity-rich regions in Maremmana Semi-Feral Cattle using pedigree and genomic data. *Animals*, *10*, 2285.

Bizarria dos Santos, W., Pimenta Schettini, G., Fonseca, M. G., Pereira, G. L., Loyola Chardulo, L. A., Rodrigues Machado Neto, O., Baldalssini, W. A., Nunes de Oliveira, H., & Abdallah Curi, R. (2021). Fine-scale estimation of inbreeding rates, runs of homozygosity and genome-wide heterozygosity levels in the Mangalarga Marchador horse breed. *Journal of Animal Breeding and Genetics*, *138*, 61–173.

Blasco, A., Martínez-Álvaro, M., García, M. L., Ibáñez-Escriche, N., & Argente, M. J. (2017). Selection for environmental variance of litter size in rabbits. *Genetics Selection Evolution*, *49*, 48.

Bolet, G., Garreau, H., Joly, T., Theau-Clement, M., Falieres, J., Hurtaud, J., & Bodin, L. (2007). Genetic homogenisation of birth weight in rabbits: Indirect selection response for uterine horn characteristics. *Livestock Science*, *111*, 28–32.

Boyko, A. R., Quignon, P., Li, L., Schoenebeck, J. J., Degenhardt, J. D., Lohmueller, K. E., Zhao, K., Brisbin, A., Parker, H. G., von Holdt, B. M., Cargill, M., Auton, A., Reynolds, A., Elkahloun, A. G., Castelhano, M., Mosher, D. S., Sutter, N. B., Johnson, G. S., Novembre, J., … Ostrander, E. A. (2010). A simple genetic architecture underlies morphological variation in dogs. *PLOS Biology*, *10*, e1000451.

Broom, D. M. (2008). Welfare assessment and relevant ethical decisions: Key concepts. *Annual Review of Biomedical Sciences*, *10*, T79–T90.

Caivio-Nasner, S., López-Herrera, A., González-Herrera, L. G., & Rincón, J. C. (2021). Diversity analysis, runs of homozygosity and genomic inbreeding reveal recent selection in Blanco Orejinegro cattle. *Journal of Animal Breeding and Genetics*, *138*, 613–627.

Casto-Rebollo, C., Argente, M. J., García, M. L., Blasco, A., & Ibáñez-Escriche, N. (2021). Selection for environmental variance of litter size in rabbits involves genes in pathways controlling animal resilience. *Genetic Selection Evolution*, *53*, 59.

Ceballos, F. C., Joshi, P. K., Clark, D. W., Ramsay, M., & Wilson, J. F. (2018). Runs of homozygosity: Windows into population history and trait architecture. *Nature Reviews Genetics*, *19*, 220–234.

Chang, C. C., Chow, C. C., Tellier, L. C., Vattikuti, S., Purcell, S. M., & Lee, J. J. (2015). Second-generation PLINK: Rising to the challenge of larger and richer datasets. *GigaScience*, *4*, 7.

Cortellari, M., Bionda, A., Negro, A., Frattini, S., Mastrangelo, S., Somenzi, E., Lasagna, E., Sarti, F. M., Ciampolini, R., Marletta, D., Liotta, L., Marsan, A. M., Pilla, F., Colli, L., Talenti, A., & Crepaldi, P. (2021). Runs of homozygosity in the Italian goat breeds: Impact of management practices in low-input systems. *Genetics Selection Evolution*, *53*, 92.

Curik, I., Ferenčaković, M., & Sölkner, J. (2014). Inbreeding and runs of homozygosity: A possible solution to an old problem. *Livestock Science*, *166*, 26–34.

Doekes, H. P., Veerkamp, R. F., Bijma, P., de Jong, G., Hiemstra, S. J., & Windig, J. J. (2019). Inbreeding depression due to recent and ancient inbreeding in Dutch Holstein–Friesian dairy cattle. *Genetics Selection Evolution*, *51*, 54.

dos Santos Daltro, D., Pagung Ambronisis, D., Negri, D., Vinícius, M., Barbosa da Silva, G., & Araújo Cobuci, J. (2022). Reaction

norm model to describe environmental sensitivity in Girolando cattle. *Livestock Science*, *263*, 105025.

Druml, T., Neuditschko, M., Grilz-Seger, G., Horna, M., Ricard, A., Mesarič, M., Cotman, M., Pausch, H., & Brem, G. (2018). Population networks associated with runs of homozygosity reveal new insights into the breeding history of the Haflinger Horse. *Journal of Heredity*, *109*, 384–392.

Elbeltagy, A. R., Bertolini, F., Fleming, D. S., van Goor, A., Ashwel, L. C. M., Schmidt, C. J., Kugonza, D. R., Lamont, S. J., & Rothschild, M. F. (2019). Natural selection footprints among African chicken breeds and village ecotypes. *Frontiers in Genetics*, *10*, 376.

Ferenčaković, M., Sölkner, J., & Curik, I. (2013). Estimating autozygosity from high-throughput information: Effects of SNP density and genotyping errors. *Genetics Selection Evolution*, *45*, 42.

Fernández, B. J., & Toro, M. A. (1999). The use of mathematical programming to control inbreeding in selection schemes. *Journal of Animal Breeding and Genetics*, *116*, 447–466.

Formoso-Rafferty, N., Cervantes, I., Ibáñez-Escriche, N., & Gutiérrez, J. P. (2016a). Genetic control of the environmental variance for birth weight in seven generations of a divergent selection experiment in mice. *Journal of Animal Breeding and Genetics*, *133*, 227–237.

Formoso-Rafferty, N., Cervantes, I., Ibáñez-Escriche, N., & Gutiérrez, J. P. (2016b). Correlated genetic trends for production and welfare traits in a mouse population divergently selected for birth weight environmental variability. *Animal*, *10*, 1770–1777.

Formoso-Rafferty, N., Cervantes, I., Ibáñez-Escriche, N., & Gutiérrez, J. P. (2017). Modulating birth weight heritability in mice. *Journal of Animal Science*, *95*, 531.

Formoso-Rafferty, N., Cervantes, I., Sánchez, J. P., Gutiérrez, J. P., & Bodin, L. (2019). Effect of feed restriction on the environmental variability of birth weight in divergently selected lines of mice. *Genetics Selection Evolution*, *51*, 27.

Formoso-Rafferty, N., Chavez, K., Ojeda, C., Cervantes, I., & Gutiérrez, J. P. (2020). Selection response in a divergent selection experiment for birth weight variability in mice compared with a control line. *Animals*, *10*, 920.

Formoso-Rafferty, N., El-Ouazizi El-Kahia, L., Arias-Álvarez, M., Gutiérrez, J. P., & Cervantes, I. (2023). Embryo survival and fertility differ in lines divergently selected for birth weight homogeneity in mice. *Journal of Animal Breeding and Genetics*, *140*, 549–557.

Formoso-Rafferty, N., Gutiérrez, J. P., García-Álvarez, A., Pérez, T., & Cervantes, I. (2022). Impact of selection for birth weight variability on reproductive longevity: A mice model. *Journal of Animal Breeding and Genetics*, *139*, 370–379.

Fox, J., & Weisberg, S. (2019). *An R companion to applied regression* (3rd ed.). Sage.

Ganteil, A., Rodriguez-Ramilo, S. T., Ligonesche, B., & Larzul, C. (2020). Characterization of autozygosity in pigs in three-way crossbreeding. *Frontiers in Genetics*, *11*, 584556.

Garreau, H., Bolet, G., Larzul, C., Robert-Granié, C., Saleil, G., SanCristobal, M., & Bodin, L. (2008). Results of four generations of a canalising selection for rabbit birth weight. *Livestock Science*, *119*, 55–62.

Grilz-Seger, G., Druml, T., Neuditschko, M., Mesarič, M., Cotman, M., & Brem, G. (2019). Analysis of ROH patterns in the Noriker horse breed reveals signatures of selection for coat color and body size. *Animal Genetics*, *50*, 334–346.

Gutiérrez, J. P., & Goyache, F. (2005). A note on ENDOG: A computer program for analysing pedigree information. *Journal of Animal Breeding and Genetics*, *122*, 172–176.

Gutiérrez, J. P., Nieto, B., Piqueras, P., Ibáñez, N., & Salgado, C. (2006). Genetic parameters for canalisation analysis of litter size and litter weight traits at birth in mice. *Genetics Selection Evolution*, *38*, 445–462.

Howard, J. T., Pryce, J. E., Baes, C., & Maltecca, C. (2017). Invited review: Inbreeding in the genomics era: Inbreeding, inbreeding depression, and management of genomic variability. *Journal of Dairy Science*, *100*, 6009–6024.

Howrigan, D. P., Simonson, M. A., & Keller, M. C. (2011). Detecting autozygosity through runs of homozygosity: A comparison of three autozygosity detection algorithms. *BMC Genomics*, *12*, 460.

Ibáñez-Escriche, N., Moreno, A., Nieto, B., Piqueras, P., Salgado, C., & Gutiérrez, J. P. (2008). Genetic parameters related to environmental variability of weight traits in a selection experiment for weight gain in mice: Signs of correlated canalised response. *Genetics Selection Evolution*, *40*, 279–293.

Joaquim, L. B., Chu, T. C. S., Marchesi, J. A. P., Savegnago, R. P., Buzanskas, M. E., Zanella, R., Cantão, M. E., Peixoto, J. O., Ledur, M. C., Irgang, R., & Munari, D. P. (2019). Genomic structure of a crossbred Landrace pig population. *PLoS One*, *14*, e0212266.

Kim, E., Cole, J., Huson, H., Wiggans, G. R., van Tassel, C. P., Crooker, G. L., Da, Y., & Sonstegard, T. S. (2013). Effect of artificial selection on runs of homozygosity in U.S. Holstein Cattle. *PLoS One*, *8*, E80813.

Lerner, I. M. (1954). *Genetic homeostasis*. Oliver and Boyd.

Lewontin, R. C. (1964). Selection in and of populations. In J. A. Moore (Ed.), *Ideas in modern biology natural history press* (pp. 299–311). Natural History Press.

Lozada-Soto, E. A., Tiezzi, F., Jiang, J., Cole, J. B., VanRaden, P. M., & Maltecca, C. (2022). Genomic characterization of autozygosity and recent inbreeding trends in all major breeds of US dairy cattle. *Journal of Dairy Science*, *105*, 8956–8971.

Marchesi, J. A. P., Buzanskas, M. E., Cantão, M. E., Ibelli, A. M. G., Peixoto, J. O., Joaquim, L. B., Moreira, G. C. M., Godoy, T. F., Sbardella, A. P., Figueiredo, E. A. P., Coutinho, L. L., Munari, D. P., & Ledur, M. C. (2018). Relationship of runs of homozygosity with adaptive and production traits in a paternal broiler line. *Animal*, *12*, 1126–1134.

Marjanovic, J., Mulder, H. A., Khaw, H. L., & Bijma, P. (2016). Genetic parameters for uniformity of harvest weight and body size traits in the GIFT strain of Nile tilapia. *Genetics Selection Evolution*, *48*, 41.

Marras, G., Gaspa, G., Sorbolini, S., Dimauro, C., Ajmone-Marsan, P., Valentini, A., Williams, J. L., & Macciotta, N. P. (2015). Analysis of runs of homozygosity and their relationship with inbreeding in five cattle breeds farmed in Italy. *Animal Genetics*, *46*, 110–121.

Mastrangelo, S., Biscarini, F., Auzino, B., Ragatzu, M., Spaterna, A., & Ciampolini, R. (2018). Genome-wide diversity and runs of homozygosity in the "Braque Français, type Pyrénées" dog breed. *BMC Research Notes*, *11*, 13.

McQuillan, R., Leutenegger, A. L., Abdel-Rahman, R., Franklin, C. S., Pericic, M., Barac-Lauc, L., Smolej-Narancic, N., Janicijevic, B., Polasek, O., Tenesa, A., Macleod, A. K., Farrington, S.

M., Rudan, P., Hayward, C., Vitart, V., Rudan, I., Wild, S. H., Dunlop, M. G., Wright, A. F., … Wilson, J. F. (2008). Runs of homozygosity in European populations. *The American Journal of Human Genetics*, *83*, 359–372.

Meuwissen, T., & Luo, Z. (1992). Computing inbreeding coefficients in large populations. *Genetics Selection Evolution*, *24*, 305–313.

Meyermans, R., Gorssen, W., Buys, N., & Janssens, S. (2020). How to study runs of homozygosity using PLINK? A guide for analyzing medium density SNP data in livestock and pet species. *BMC Genomics*, *21*, 94.

Mooney, J. A., Yohannes, A., & Lohmueller, K. E. (2021). The impact of identity by descent on fitness and disease in dogs. *Proceedings of the National Academy of Sciences*, *118*, e2019116118.

Moreno, A., Ibáñez-Escriche, N., García-Ballesteros, S., Salgado, C., Nieto, B., & Gutiérrez, J. P. (2012). Correlated genetic trend in the environmental variability of weight traits in mice. *Livestock Science*, *148*, 189–195.

Mulim, H. A., Brito, L. F., Pinto, L. F. B., Ferraz, J. B. S., Grigoletto, L., Silva, M. R., & Pedrosa, V. B. (2022). Characterization of runs of homozygosity, heterozygosity-enriched regions, and population structure in cattle populations selected for different breeding goals. *BMC Genomics*, *23*, 209.

Nosrati, M., Asadollahpour Nanaei, H., Javanmard, A., & Esmailizadeh, A. (2021). The pattern of runs of homozygosity and genomic inbreeding in world-wide sheep populations. *Genomics*, *113*, 1407–1415.

Onzima, R. B., Upadhyay, M. R., Doekes, H. P., Brito, L. F., Bosse, M., Kanis, E., Groenen, M. A. M., & Crooijmans, R. P. M. A. (2018). Genome-wide characterization of selection signatures and runs of homozygosity in Ugandan goat breeds. *Frontiers in Genetics*, *9*, 318.

Peripolli, E., Munari, D. P., Silva, M. V. G. B., Lima, A. L. F., Irgang, R., & Baldi, F. (2017). Runs of homozygosity: Current knowledge and applications in livestock. *Animal Genetics*, *48*, 255–271.

Peripolli, E., Stafuzza, N. B., Amorim, S. T., de Lemos, M. V. A., Grigoletto, L., Kluska, S., Ferraz, J. B. S., Eler, J. P., Mattos, E. C., & Baldi, F. (2020). Genome-wide scan for runs of homozygosity in the composite Montana Tropical® beef cattle. *Journal of Animal Breeding and Genetics*, *137*, 155–165.

Poigner, J., Szendrö, Z., Lévai, A., Radnai, I., & Biró-Nemeth, E. (2000). Effect of birth weight and litter size on growth and mortality in rabbits. *World Rabbit Science*, *8*, 17–22.

Poyato-Bonilla, J., Sánchez-Guerrero, M. J., Cervantes, I., Gutiérrez, J. P., & Valera, M. (2021). Genetic parameters for canalization analysis of morphological traits in the Pura Raza Español horse. *Journal of Animal Breeding and Genetics*, *138*, 482–490.

Pryce, J. E., Haile-Mariam, M., Goddard, M. E., & Hayes, B. J. (2014). Identification of genomic regions associated with inbreeding depression in Holstein and Jersey dairy cattle. *Genetics Selection Evolution*, *46*, 71.

Pun, A., Cervantes, I., Nieto, B., Salgado, C., Pérez-Cabal, M. A., Ibáñez-Escriche, N., & Gutiérrez, J. P. (2013). Genetic parameters for birthweight environmental variability in mice. *Journal of Animal Breeding and Genetics*, *130*, 404–414.

Purcell, S., Neale, B., Todd-Brown, K., Thomas, L., Ferreira, M. A., Bender, D., Maller, J., Sklar, P., de Bakker, P. I., Daly, M. J., & Sham, P. C. (2007). PLINK: A tool set for whole-genome association and population-based linkage analyses. *The American Journal of Human Genetics*, *81*, 559–575.

Purfield, D. C., Berry, D. P., McParland, S., & Bradley, D. G. (2012). Runs of homozygosity and population history in cattle. *BMC Genetics*, *13*, 70.

Purfield, D. C., McParland, S., Wall, E., & Berry, D. P. (2017). The distribution of runs of homozygosity and selection signatures in six commercial meat sheep breeds. *PLoS One*, *12*, e0176780.

Rodríguez-Ramilo, S. T., Elsen, J. M., & Legarra, A. (2019). Inbreeding and effective population size in French dairy sheep: Comparison between genomic and pedigree estimates. *Journal of Dairy Science*, *102*, 4227–4237.

Rodríguez-Ramilo, S. T., Reverter, A., & Legarra, A. (2021). Islands of runs of homozygosity indicate selection signatures in *Ovis aries* 6 (OAR6) of French dairy sheep. *JDS Communications*, *2*, 132–136.

Rönnegård, L., Felleki, M., Fikse, W. F., Mulder, H. A., & Strandberg, E. (2013). Variance component and breeding value estimation for genetic heterogeneity of residual variance in Swedish Holstein dairy cattle. *Journal of Dairy Science*, *96*, 2627–2636.

Sams, A. J., & Boyko, A. R. (2019). Fine-scale resolution of runs of homozygosity reveal patterns of inbreeding and substantial overlap with recessive disease genotypes in domestic dogs. *G3 Genes|Genomes|Genetics*, *9*, 117–123.

Saura, M., Fernández, A., Varona, L., Fernández, A. I., de Cara, M. Á., Barragán, C., & Villanueva, B. (2015). Detecting inbreeding depression for reproductive traits in Iberian pigs using genome-wide data. *Genetics Selection Evolution*, *47*, 1.

Schäler, J., Krüger, B., Thaller, G., & Hinrichs, D. (2020). Comparison of ancestral, partial, and genomic inbreeding in a local pig breed to achieve genetic diversity. *Conservation Genetics Resources*, *12*, 77–86.

Schiavo, G., Bovo, S., Bertolini, F., Tinarelli, S., Dall'Olio, S., Nanni Costa, L., Gallo, M., & Fontanesi, L. (2020). Comparative evaluation of genomic inbreeding parameters in seven commercial and autochthonous pig breeds. *Animal*, *14*, 910–920.

Schiavo, G., Bovo, S., Ribani, A., Moscatelli, G., Bonacini, M., Prandi, M., Mancin, E., Mantovani, R., Dall'Olio, S., & Fontanesi, L. (2022). Comparative analysis of inbreeding parameters and runs of homozygosity islands in 2 Italian autochthonous cattle breeds mainly raised in the Parmigiano-Reggiano cheese production region. *Journal of Dairy Science*, *105*, 2408–2425.

Signer-Hasler, H., Henkel, J., Bangerter, E., Bulut, Z., VarGoats Consortium, Drögemüller, C., Leeb, T., & Flury, C. (2022). Runs of homozygosity in Swiss goats reveal genetic changes associated with domestication and modern selection. *Genetics Selection Evolution*, *54*, 6.

Soh, P. X. Y., Hsu, W. T., Khatkar, M. S., & Williamson, P. (2021). Evaluation of genetic diversity and management of disease in Border Collie dogs. *Scientific Reports*, *11*, 6243.

Strillacci, M. G., Marelli, S. P., & Martinez-Velazquez, G. (2020). Hybrid versus autochthonous Turkey populations: Homozygous genomic regions occurrences due to artificial and natural selection. *Animals*, *10*, E1318.

Vandenplas, J., Bastin, C., Gengler, N., & Mulder, H. A. (2013). Genetic variance in micro-environmental sensitivity for milk and milk quality in Walloon Holstein cattle. *Journal of Dairy Science*, *96*, 5977–5990.

Yoshida, G. M., Cáceres, P., Marín-Nahuelpi, R., Koop, B. F., & Yáñez, J. M. (2020). Estimates of autozygosity through runs of homozygosity in farmed Coho Salmon. *Genes*, *11*, 490.

Zhang, Q., Guldbrandtsen, B., Bosse, M., Lund, M. S., & Sahana, G. (2015). Runs of homozygosity and distribution of functional variants in the cattle genome. *BMC Genomics*, *16*, 542.

Zhivotovsky, L. A., & Feldman, M. W. (1992). On the difference between mean and optimum of quantitative characters under selection. *Evolution*, *46*, 1574–1578.

SUPPORTING INFORMATION

Additional supporting information can be found online in the Supporting Information section at the end of this article.

How to cite this article: Ojeda-Marín, C., Gutiérrez, J. P., Formoso-Rafferty, N., Goyache, F., & Cervantes, I. (2024). Differential patterns in runs of homozygosity in two mice lines under divergent selection for environmental variability for birth weight. *Journal of Animal Breeding and Genetics*, *141*, 193–206. https://doi.org/10.1111/jbg.12835